Research Article

Seyed Morteza Naghib, Farahnaz Behzad, Mehdi Rahmanian, Yasser Zare*, and Kyong Yop Rhee*

A highly sensitive biosensor based on methacrylated graphene oxide-grafted polyaniline for ascorbic acid determination

https://doi.org/10.1515/ntrev-2020-0061
received June 29, 2020; accepted August 05, 2020

Abstract: Functionalized graphene-based nanocomposites have opened new windows to address some challenges for increasing the sensitivity, accuracy and functionality of biosensors. Polyaniline (PANI) is one of the most potentially promising and technologically important conducting polymers, which brings together the electrical features of metals with intriguing properties of plastics including facile processing and controllable chemical and physical properties. PANI/graphene nanocomposites have attracted intense interest in various fields due to unique physicochemical properties including high conductivity, facile preparation and intriguing redox behavior. In this article, a functionalized graphene-grafted nanostructured PANI nanocomposite was applied for determining the ascorbic acid (AA) level. A significant current response was observed after treating the electrode surface with methacrylated graphene oxide (MeGO)/PANI nanocomposite. The amperometric responses showed a robust linear range of 8–5,000 μM and detection limit of 2 μM ($N = 5$). Excellent sensor selectivity was demonstrated in the presence of electroactive components interfering species, commonly found in real serum samples. This sensor is a promising candidate for rapid and selective determination of AA.

Keywords: polyaniline, methacrylated graphene oxide, nanocomposite, electrochemical biosensor, ascorbic acid

*** Corresponding author: Yasser Zare,** Department of Interdisciplinary Technologies, Biomaterials and Tissue Engineering Research Group, Breast Cancer Research Center, Motamed Cancer Institute, ACECR, Tehran, Iran, e-mail: y.zare@aut.ac.ir
*** Corresponding author: Kyong Yop Rhee,** Department of Mechanical Engineering, College of Engineering, Kyung Hee University, Yongin, 446-701, Republic of Korea, e-mail: rheeky@khu.ac.kr
Seyed Morteza Naghib: Nanotechnology Department, School of Advanced Technologies, Iran University of Science and Technology, Tehran, Iran
Farahnaz Behzad: Research institute of bioscience and biotechnology, University of Tabriz, Tabriz, Iran
Mehdi Rahmanian: Department of Interdisciplinary Technologies, Biomaterials and Tissue Engineering Research Group, Breast Cancer Research Center, Motamed Cancer Institute, ACECR, Tehran, Iran

1 Introduction

Biosensors have attracted much attention due to their unique properties such as simple procedure, easy production, fast response and cost efficiency [1–3]. Polyaniline (PANI) is a semi-flexible conducting polymer of the organic semiconductor family [4], which has attracted intensive interest as a result of remarkable features including superior conductivity [5], environmental stability [6], intriguing redox process [7] and inexpensive starting material [8]. In multidisciplinary areas, various applications for PANI have been reported such as biosensors, supercapacitors, biofuel cells, actuators, corrosion protection, membranes, solar cell devices, and rechargeable batteries [4,9–12]. Tunable properties, good processability (facile synthesis process), affordability, suitable electrochemical and environmental stability, strong bimolecular interactions and intriguing acid/base and doping/dedoping properties have made PANI a promising polymer among inherently conducting polymers [10].

Graphene, a single layer of carbon atoms with sp^2 chemical bonds, is the base for all nanoscale carbon materials such as fluorine bucky balls and carbon nanotubes (CNTs) [13–20]. Simple production procedures in comparison with other carbon nanomaterials and several properties, including zero band gap, high conductivity, flexibility, exceptional chemical stability, extremely wide porous structure, high specific surface area, high mobility of charge carriers and cost efficiency, make the graphene a promising nanomaterial for the next era [21]. Graphene-based materials have been extensively used in biosensor applications due to their exceptional electrical, electrochemical and optical characteristics [22,23].

Nanocomposites have attracted much attention due to their exceptional properties [17,24–41]. Mechanical performance and electrical conductivity are the main characteristics that are developed with the combination of various materials into a nanocomposite [42–46]. Recently, conductive nanocomposites have captured the great interest in bioelectronics and biosensing fields [47]. Among them, graphene-grafted PANI nanocomposites are valuable owing to their excellent characteristics [48–50]. Combination of conducting polymers into a conductive nanostructure enhances the capacity, sensitivity, selectivity and electrical conductivity depending on the preparation methods and morphology. There are π-conjugated electrons in both graphene and PANI. These composites possessed several features including enhanced mechanical strength and excellent electrical conductivity [51]. Also, graphene-grafted PANI nanocomposites are utilized for preparing the electrode substrates. Recently, graphene-grafted PANI nanocomposites with excellent electrochemical characteristics and great conductivity have been utilized for numerous purposes such as biosensors, energy storage tools and electrochemical devices [6].

Ascorbic acid (AA), a reducing agent and successful antioxidant, plays some roles in preventing radical-induced ailments such as tumors and neurodegenerative [14,52]. The deficiency of AA can cause scrubbing, whereas its overdose can lead to stomach cramps and diarrhea [53]. The determination of AA levels is critical for diagnosis of food ingredients. There is a crucial necessity for determining AA level for healthcare and food quality/security due to the healthiness and industrial worth of AA and its low dose in biological and food samples [52].

Electrochemical methods have established rapid and low-cost performance as well as fast response with high selectivity, stability and sensitivity in determining some biomolecules and analytes [54]. Nanostructured composites such as palladium (Pd) nanowire-modified graphene [55], multiwall CNTs dispersed in polyhistidine [56], Fe_3O_4@gold (Au)-loaded graphene [57] and ZnO nanowire on hierarchical graphene [58] were reported for developing the sensitivity and selectivity of AA. Moreover, other nanocomposites including graphene-grafted PANI [52], graphene-supported platinum (Pt) nanoparticles [59], over-oxidized polypyrrole, PdNPs/Au [60] and 3D graphene foam CuO nanoflowers [61] have been exploited for determining AA.

Our group previously synthesized NFG/AgNPs/PANI for AA biosensing, which was more complex and expensive [52]. Moreover, we synthesized methacrylated graphene oxide (MeGO)/PANI nanocomposite and characterized it by physiochemical and electrochemical tests [6]. In this study, a simpler nanocomposite based on MeGO-grafted PANI is applied as electrochemical biosensor that has several benefits including cost efficiency, high sensitivity and good selectivity over AA determination. The linear range and detection limit of the sensing device are 8–5,000 and 2 μM, respectively. This platform shows the excellent stability over electroactive compounds.

2 Materials and methods

2.1 Chemicals

The potassium ferricyanide ($K_3Fe(CN)_6$), potassium permanganate ($KMnO_4$), sulfuric acid (H_2SO_4), potassium nitrate (KNO_3), sodium nitrate ($NaNO_3$) and graphite fine powder (spectroscopic grade, particle size ≤50 μm) were obtained from Merck. Aniline (99%), dimethylformamide, phosphate-buffered saline (PBS), *N*-hydroxysuccinimide and 1-ethyl-3-(3-dimethylamino-propyl) carbodiimide hydrochloride were purchased from Sigma.

2.2 Synthesis of MeGO

Graphite oxide was synthesized via the modified Hummer method [62]. Then, MeGO nanomaterials were prepared based on our previous studies [21,49].

2.3 MeGO-grafted FTO electrode

For preparing the amended electrode substrate, FTO glass plates (8 resistance) with the surface area of 0.25 cm^2 were provided and sequential ultrasonic cleaning was performed for 10 min in isopropanol, ethanol, acetone and deionized (DI) water. Under Ar gas flow, the FTO sheets were dried. Then, MeGO suspended in DI was deposited (20, 30 and 40 μL) on the FTO surface by the cast coating method, and it was allowed to dry at 45°C, and the optimum volume was selected (40 µL).

2.4 Electropolymerization of aniline

Electropolymerization of PANI on the electrode surface was established according to our previous study [6]. Briefly, electrodepositing PANI on the MeGO-grafted FTO was initiated with 20 successive cyclic voltammograms (CVs) in a solution consisting of 0.03 M aniline monomer. Then, 0.5 M H_2SO_4 was applied on the electrode surface.

3 Results and discussion

Transmission electron microscopy (TEM) and field emission scanning electron microscopy (FESEM) tests were applied for investigating the morphology, topography and uniformity of the functionalized MeGO and MeGO/PANI nanocomposite. Figure 1a depicts the TEM image demonstrating a very thin layer of MeGO. The MeGO synthesized in this research was more transparent and uniform in comparison with previous works [63]. Based on previous results, the graphene nanosheets with excellent transparency had flake-like shapes and wrinkles and were more stable upon the exposure to the electron beam.

Figure 1b shows the microstructure of MeGO/PANI sample by the FESEM analysis. A porous structure was observed after electropolymerization of PANI on the MeGO surface. The forming of the pellet/flake-like microstructure and variations in the topography and morphology of the MeGO substrate corroborated the formation of PANI on the surface (Figure 1b). Clearly, the black regions and transparent edges were ascribed to PANI and MeGO nanosheets in MeGO/PANI nanocomposite, respectively. AA, an important factor for the synthesis and maintenance of collagen in tissue regeneration [64], was tested on our biosensor to assess its performance. CVs of the electrode modified with MeGO/PANI nanocomposites were conducted in the absence and the presence of AA (Figure 2). The results showed the highest catalytic effect for the AA solution.

To obtain the reaction mechanism of AA with the electrode surface, the changes in the oxidation peak of AA in the nanocomposite electrode were examined at

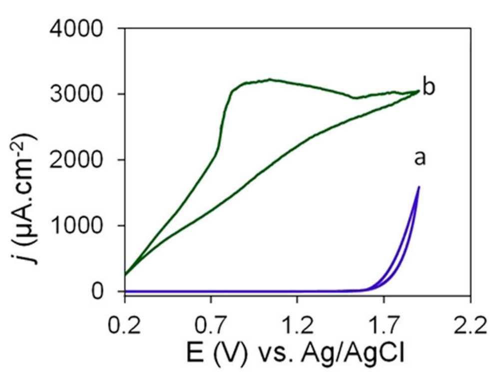

Figure 2: CVs of (a) MeGO/PANI in 0.02 M PBS without AA and (b) with 10 mM AA at the scan rate of 100 mV s^{-1}.

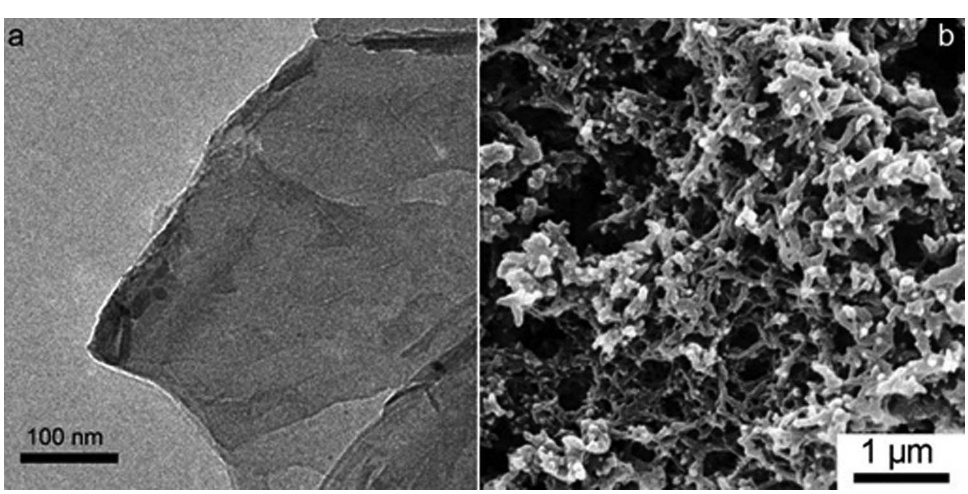

Figure 1: The morphology and uniformity of the amended electrodes: (a) TEM and (b) FESEM images of the MeGO and pellet/flake-like MeGO/PANI, respectively.

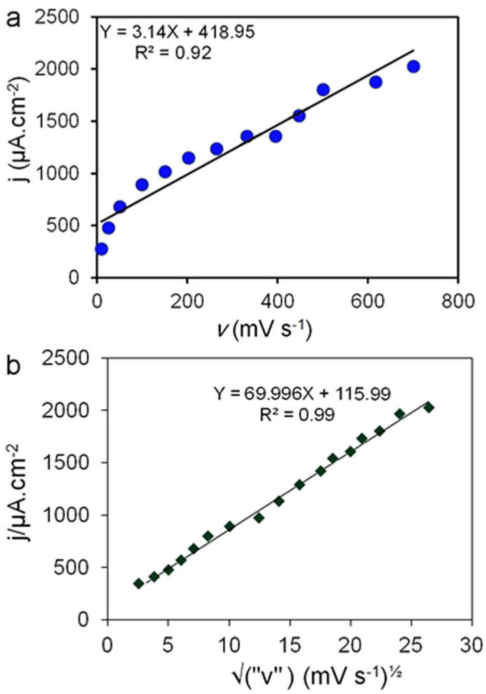

Figure 3: The plots of (a) scan rate and (b) peak current versus scan rate ½.

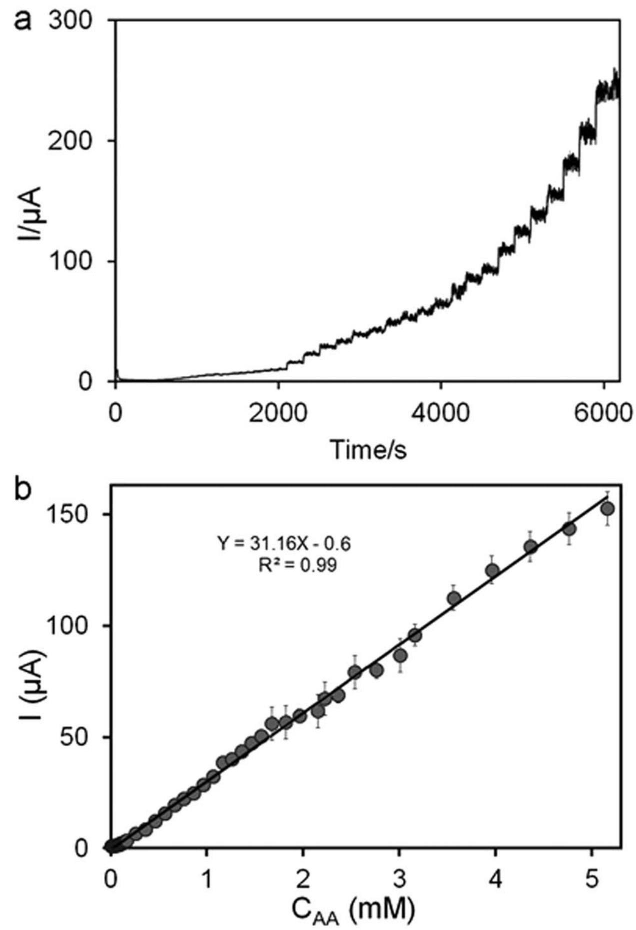

Figure 4: Calibration curve and amperometric responses (linear range) of the MeGO/PANI-functionalized biosensor for determining AA and investigating the surface redox reaction. Applied potential was +0.8 V.

different scan rates. The increase of scan rates from 10 to 700 mV s^{-1} slightly changed the oxidation peak potentials (Figure 3). AA oxidation peak current versus scan rate ½ with higher regression coefficient is linear. This indicates that the reaction mechanisms of AA with the electrode surface follow the diffusion mechanism. Moreover, the peak potential shifts to more positive potential with the increasing scan rate, which is another sign for the diffusion mechanism of AA on the electrode surface. Oxidation peak potential of AA catalysis was selected for chronoamperometry techniques to obtain the linear range of the sensor.

Successive aliquots of increasing concentrations of AA were tested on the sensor to obtain amperometric responses of the nanocomposite-modified electrodes. The electrode shows amperometric responses proportional to the AA concentration. The MeGO/PANI electrode demonstrates higher current (less uniform response) along with higher noise compared to MeGO electrode at the same concentrations of AA. This can be attributed to the active edges of graphene, which result in better interactions with AA. The nanocomposite electrode presents greater stability than MeGO electrode.

Figure 4a depicts the current increase in AA level from 8 to 5,000 µM in 0.02 M PBS (pH = 7.4). A linear trend is observed between the peak current and the AA level in Figure 4b (with a correlation of R^2 = 0.99). The detection limit of the amperometric responses was evaluated to be 2 µM (S/N = 5). Therefore, by addition of the AA aliquot (dropwise) to the PBS buffer, the current response (output) of the nanocomposite-based biosensor dramatically promotes to the AA redox reaction linearly with analyte biosensing enviable range. As given in Table 1, the electroanalytic and sensing features of the functionalized MeGO/PANI nanocomposite are meaningfully more than the AA biosensors from the previous reports. Some samples have low detection limit, while others show wide linear sensing range. In comparison with other studies, our sensing device shows very low detection limit and wide linear range. Therefore, this strategy for developing an analytical device could be established as a promising protocol to promote the sensing performance.

Table 1: The comparison of the linear range and detection limit of the present study with others

Electrode materials	Detection limit (μM)	Linear range (μM)	Ref.
PANI/PSS/Gr	5	100–1,000	[65]
NG	2.2	5–1,300	[66]
CoPc–MWCNTs	1	10–2,600	[67]
AGCE/ASOD	2	5–400	[68]
PdNi/C	0.5	10–1,800	[69]
MWCNT/CCE	7.71	15–800	[70]
Pt-Au hybrid	103	103–165	[71]
Chitosan-graphene	50	50–1,200	[72]
OMC/Nafion	20	40–800	[73]
ZnO/RM	1.4	15–240	[74]
MBMOR/P	12.1	20–800	[75]
Pd/CNFs	15	50–4,000	[76]
PMPy/Pd	1,000	50–1,000	[77]
DB71	1	1–2,000	[78]
$BPPF_6$/CPE	8	10–3,000	[79]
PPF/GNS	120	400–6,000	[80]
PdNPs-GO	—	20–2,280	[81]
Pt/Au/GCE	—	24–384	[71]
NFG/AgNPs (1, 90 s)/PANI	8	10–5,460	[52]
NFG/AgNPs (10, 90 s)/PANI	50	50–11,460	[52]
MeGO/PANI	2	8–5,000	Present work

The selectivity of the MeGO/PANI nanocomposite was evaluated in the presence of some interferences. The current responses of the interfering species were also analyzed at the modified electrode. The selectivity of the sensor was tested in PBS 0.02 M (pH = 7.4) with 10 mM interferences and 5 mM AA. As shown in Figure 5, a significant current response was observed for AA redox reaction, while interferences could not influence the current responses. In spite of the high concentrations of interferences, negligible changes were sensed in the sensing outputs, demonstrating the excellent selectivity of the present platform upon AA determination.

4 Conclusions

The functionalized MeGO/PANI nanocomposite demonstrated an excellent sensing activity over AA redox reaction. The linear sensing range and the detection limit of the sensing platform were dramatically more than most cases. Electroanalytical and biosensing results illustrated that the combination of MeGO as a 2D

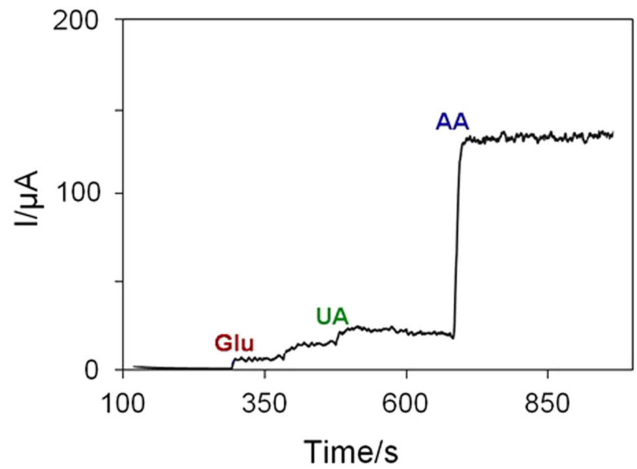

Figure 5: The selectivity of MeGO/PANI sensor in the existence of 10 mM of uric acid and glucose and 5 mM of the analyte in 0.02 M PBS. The applied potential was 0.8 V (versus Ag/AgCl).

nanostructure and PANI as a familiar conducting polymer played a significant role in bioelectrochemical sensing applications. AA was scrutinized as a bioanalyte for verifying the declaration. The time-dependent amperometric output of the MeGO/PANI nanocomposite was noteworthy in an extensive linear range. It is concluded that the present sensor is a talented candidate for quick and careful sensing of AA.

Acknowledgments: This work was supported by the Basic Science Research Program through the National Research Foundation of Korea (NRF) funded by the Ministry of Education, Science and Technology (project number: 2020R1A2B5B02002203).

Conflict of interest: The authors declare no conflict of interest regarding the publication of this paper.

References

[1] Krishnan SK, Singh E, Singh P, Meyyappan M, Nalwa HS. A review on graphene-based nanocomposites for electrochemical and fluorescent biosensors. RSC Adv. 2019;9(16):8778–881.

[2] Safavi A, Ahmadi R, Mohammadpour Z, Zhou J. Fluorescent pH nanosensor based on carbon nanodots for monitoring minor intracellular pH changes. RSC Adv. 2016;6(106):104657–64.

[3] Abi A, Mohammadpour Z, Zuo X, Safavi A. Nucleic acid-based electrochemical nanobiosensors. Biosens Bioelectron. 2018;102:479–89.

[4] Kazemi F, Naghib SM, Mohammadpour Z. Multifunctional micro-/nanoscaled structures based on polyaniline: an

overview of modern emerging devices. Mater Today Chem. 2020;16:100249.
[5] Rahimzadeh Z, Naghib SM, Zare Y, Rhee KY. An overview on the synthesis and recent applications of conducting poly(3,4-ethylenedioxythiophene) (PEDOT) in industry and biomedicine. J Mater Sci. 2020;55:7575–611.
[6] Naghib SM, Zare Y, Rhee KY. A facile and simple approach to synthesis and characterization of methacrylated graphene oxide nanostructured polyaniline nanocomposites. Nanotechnol Rev. 2020;9(1):53–60.
[7] Salahandish R, Ghaffarinejad A, Omidinia E, Zargartalebi H, Majidzadeh-A K, Naghib SM, et al. Label-free ultrasensitive detection of breast cancer miRNA-21 biomarker employing electrochemical nano-genosensor based on sandwiched AgNPs in PANI and N-doped graphene. Biosens Bioelectron. 2018;120:129–36.
[8] Salahandish R, Ghaffarinejad A, Naghib SM, Majidzadeh-A K, Zargartalebi H, Sanati-Nezhad A. Nano-biosensor for highly sensitive detection of HER2 positive breast cancer. Biosens Bioelectron. 2018;117:104–11.
[9] Yusoff II, Rohani R, Ng LY, Mohammad AW. Conductive polyelectrolyte multilayers PANI membranes synthesis for tunable filtration ranges. J Mater Sci. 2019;54(19):12988–3005.
[10] Niu F-X, Wang Y-X, Zhang Y-T, Xie S-K, Ma L-R, Wang C-G, et al. A hierarchical architecture of PANI/APTES/SiC nano-composites with tunable dielectric for lightweight and strong microwave absorption. J Mater Sci. 2019;54(3):2181–92.
[11] Miao J, Li H, Qiu H, Wu X, Yang J. Graphene/PANI hybrid film with enhanced thermal conductivity by in situ polymerization. J Mater Sci. 2018;53(12):8855–65.
[12] Almasi-Kashi M, Mokarian MH, Alikhanzadeh-Arani S. Improvement of the microwave absorption properties in FeNi/PANI nanocomposites fabricated with different structures. J Alloy Compd. 2018;742:413–20.
[13] Rostami A, Moosavi MI. High-performance thermoplastic polyurethane nanocomposites induced by hybrid application of functionalized graphene and carbon nanotubes. J Appl Polym Sci. 2020;137:48520.
[14] Salahandish R, Ghaffarinejad A, Naghib SM, Majidzadeh-A K, Sanati-Nezhad A. A novel graphene-grafted gold nanoparticles composite for highly sensitive electrochemical biosensing. IEEE Sens J. 2018;18(6):2513–9.
[15] Mohammadpour Z, Abdollahi SH, Omidvar A, Mohajeri A, Safavi A. Aqueous solutions of carbohydrates are new choices of green solvents for highly efficient exfoliation of two-dimensional nanomaterials. J Mol Liq. 2020;309:113087.
[16] Mohammadpour Z, Majidzadeh-A K. Applications of two-dimensional nanomaterials in breast cancer theranostics. ACS Biomater Sci Eng. 2020;6(4):1852–73.
[17] Power AC, Gorey B, Chandra S, Chapman J. Carbon nanomaterials and their application to electrochemical sensors: a review. Nanotechnol Rev. 2018;7(1):19–41.
[18] Chen W, Lv G, Hu W, Li D, Chen S, Dai Z. Synthesis and applications of graphene quantum dots: a review. Nanotechnol Rev. 2018;7(2):157–85.
[19] Jiao Z, Zhang B, Li C, Kuang W, Zhang J, Xiong Y, et al. Carboxymethyl cellulose-grafted graphene oxide for efficient antitumor drug delivery. Nanotechnol Rev. 2018;7(4):291–301.
[20] Das S, Ghosh CK, Sarkar CK, Roy S. Facile synthesis of multilayer graphene by electrochemical exfoliation using organic solvent. Nanotechnol Rev. 2018;7(6):497–508.
[21] Naghib SM. Two-dimensional functionalised methacrylated graphene oxide nanosheets as simple and inexpensive electrodes for biosensing applications. Micro Nano Lett. 2019;14(4):462–5.
[22] Askari E, Naghib SM, Seyfoori A, Maleki A, Rahmanian M. Ultrasonic-assisted synthesis and *in vitro* biological assessments of a novel herceptin-stabilized graphene using three dimensional cell spheroid. Ultrason Sonochem. 2019;58:104615.
[23] Kalkhoran AHZ, Naghib SM, Vahidi O, Rahmanian M. Synthesis and characterization of graphene-grafted gelatin nanocomposite hydrogels as emerging drug delivery systems. Biomed Phys & Eng Express. 2018;4(5):055017.
[24] Zhang P, Yi W, Xu H, Gao C, Hou J, Jin W, et al. Supramolecular interactions of poly[(9,9-dioctylfluorenyl-2,7-diyl)-co-thiophene] with single-walled carbon nanotubes. Nanotechnol Rev. 2018;7(6):487–95.
[25] Zare Y, Garmabi H, Rhee KY. Degradation-biosensing performance of polymer blend carbon nanotubes (CNTs) nanocomposites. Sens Actuators A. 2019;295:113–24.
[26] Zare Y, Rhee KY. Calculation of the electrical conductivity of polymer nanocomposites assuming the interphase layer surrounding carbon nanotubes. Polymers. 2020;12(2):404.
[27] Zare Y, Rhee KY. A multistep methodology for calculation of the tensile modulus in polymer/carbon nanotube nanocomposites above the percolation threshold based on the modified rule of mixtures. RSC Adv. 2018;8(54):30986–93.
[28] Peng W, Rhim S, Zare Y, Rhee KY. Effect of "Z" factor for strength of interphase layers on the tensile strength of polymer nanocomposites. Polym Compos. 2019;40:1117–22.
[29] Ventrapragada LK, Creager SE, Rao AM, Podila R. Carbon nanotubes coated paper as current collectors for secondary Li-ion batteries. Nanotechnol Rev. 2019;8(1):18–23.
[30] Li Z, Xu K, Pan Y. Recent development of supercapacitor electrode based on carbon materials. Nanotechnol Rev. 2019;8(1):35–49.
[31] Zare Y, Rhee KY. Effects of interphase regions and filler networks on the viscosity of PLA/PEO/carbon nanotubes biosensor. Polym Compos. 2019;40:4135–41.
[32] Kalantari E, Naghib SM, Iravani NJ, Esmaeili R, Naimi-Jamal MR, Mozafari M. Biocomposites based on hydroxyapatite matrix reinforced with nanostructured monticellite ($CaMgSiO_4$) for biomedical application: synthesis, characterization, and biological studies. Mater Sci Eng C. 2019;105:109912.
[33] Kalantari E, Naghib SM. A comparative study on biological properties of novel nanostructured monticellite-based composites with hydroxyapatite bioceramic. Mater Sci Eng C. 2019;98:1087–96.
[34] Zare Y, Rhee KY. The effective conductivity of polymer carbon nanotubes (CNT) nanocomposites. J Phys Chem Solids. 2019;131:15–21.
[35] Zare Y, Rhee KY. Tensile modulus prediction of carbon nanotubes-reinforced nanocomposites by a combined model for dispersion and networking of nanoparticles. J Mater Res Technol. 2020;9:22–32.

[36] Zare Y, Rhee KY, Park SJ. Simple model for hydrolytic degradation of poly(lactic acid)/poly(ethylene oxide)/carbon nanotubes nanobiosensor in neutral phosphate-buffered saline solution. J Biomed Mater Res Part A. 2019;107:2706–17.
[37] Zare Y, Rhee KY. A simulation work for the influences of aggregation/agglomeration of clay layers on the tensile properties of nanocomposites. JOM. 2019;71:3989–95.
[38] Roy S, Petrova RS, Mitra S. Effect of carbon nanotube (CNT) functionalization in epoxy-CNT composites. Nanotechnol Rev. 2018;7(6):475–85.
[39] Li Z, Xu K, Wei F. Recent progress on photodetectors based on low dimensional nanomaterials. Nanotechnol Rev. 2018;7(5):393–411.
[40] Lei M, Chen Z, Lu H, Yu K. Recent progress in shape memory polymer composites: methods, properties, applications and prospects. Nanotechnol Rev. 2019;8(1):327–51.
[41] Kalwar K, Shen M. Electrospun cellulose acetate nanofibers and Au-AgNPs for antimicrobial activity – a mini review. Nanotechnol Rev. 2019;8(1):246–57.
[42] Zare Y, Rhee KY. Prediction of loss factor (tan δ) for polymer nanocomposites as a function of yield tress, relaxation time and the width of transition region between Newtonian and power-law behaviors. J Mech Behav Biomed Mater. 2019;96:136–43.
[43] Zare Y, Rhee KY. Significances of interphase conductivity and tunneling resistance on the conductivity of carbon nanotubes nanocomposites. Polym Compos. 2020;41:748–56.
[44] Zare Y, Rhee KY. Study on the effects of the interphase region on the network properties in polymer carbon nanotube nanocomposites. Polymers. 2020;12(1):182.
[45] Zare Y, Garmabi H, Rhee KY. Roles of filler dimensions, interphase thickness, waviness, network fraction, and tunneling distance in tunneling conductivity of polymer CNT nanocomposites. Mater Chem Phys. 2018;206:243–50.
[46] Lee S-Y, Hwang J-G. Finite element nonlinear transient modelling of carbon nanotubes reinforced fiber/polymer composite spherical shells with a cutout. Nanotechnol Rev. 2019;8(1):444–51.
[47] Naghib SM. Fabrication of nafion/silver nanoparticles/reduced graphene nanosheets/glucose oxidase nanobiocomposite for electrochemical glucose biosensing. Anal Bioanal Electrochem. 2016;8:453–65.
[48] Li Y, Zhou M, Xia Z, Gong Q, Liu X, Yang Y, et al. Facile preparation of polyaniline covalently grafted to isocyanate functionalized reduced graphene oxide nanocomposite for high performance flexible supercapacitors. Colloids Surf A. 2020;125172.
[49] Mamaghani KR, Naghib SM, Zahedi A, Kalkhoran AHZ, Rahmanian M. Fast synthesis of methacrylated graphene oxide: a graphene-functionalised nanostructure. Micro Nano Lett. 2018;13(2):195–7.
[50] Mamaghani KR, Naghib SM, Zahedi A, Rahmanian M, Mozafari M. GelMa/PEGDA containing graphene oxide as an IPN hydrogel with superior mechanical performance. Mater Today Proc. 2018;5(7):15790–9.
[51] Lou C, Jing T, Zhou J, Tian J, Zheng Y, Wang C, et al. Laccase immobilized polyaniline/magnetic graphene composite electrode for detecting hydroquinone. Int J Biol Macromolecules. 2020;149:1130–8.
[52] Salahandish R, Ghaffarinejad A, Naghib SM, Niyazi A, Majidzadeh-A K, Janmaleki M, et al. Sandwich-structured nanoparticles-grafted functionalized graphene based 3D nanocomposites for high-performance biosensors to detect ascorbic acid biomolecule. Sci Rep. 2019;9(1):1–11.
[53] Hu G, Guo Y, Xue Q, Shao S. A highly selective amperometric sensor for ascorbic acid based on mesopore-rich active carbon-modified pyrolytic graphite electrode. Electrochim Acta. 2010;55(8):2799–804.
[54] Salahandish R, Ghaffarinejad A, Naghib SM, Majidzadeh-A K, Zargartalebi H, Sanati-Nezhad A. Nano-biosensor for highly sensitive detection of HER2 positive breast cancer. Biosens Bioelectron. 2018;117:104–11.
[55] Wen D, Guo S, Dong S, Wang E. Ultrathin Pd nanowire as a highly active electrode material for sensitive and selective detection of ascorbic acid. Biosens Bioelectron. 2010;26(3):1056–61.
[56] Dalmasso PR, Pedano ML, Rivas GA. Electrochemical determination of ascorbic acid and paracetamol in pharmaceutical formulations using a glassy carbon electrode modified with multi-wall carbon nanotubes dispersed in polyhistidine. Sens Actuators B. 2012;173:732–6.
[57] Liu M, Chen Q, Lai C, Zhang Y, Deng J, Li H, et al. A double signal amplification platform for ultrasensitive and simultaneous detection of ascorbic acid, dopamine, uric acid and acetaminophen based on a nanocomposite of ferrocene thiolate stabilized Fe_3O_4@Au nanoparticles with graphene sheet. Biosens Bioelectron. 2013;48:75–81.
[58] Yue HY, Huang S, Chang J, Heo C, Yao F, Adhikari S, et al. ZnO nanowire arrays on 3D hierachical graphene foam: biomarker detection of Parkinson's disease. ACS nano. 2014;8(2):1639–46.
[59] Sun C-L, Lee H-H, Yang J-M, Wu C-C. The simultaneous electrochemical detection of ascorbic acid, dopamine, and uric acid using graphene/size-selected Pt nanocomposites. Biosens Bioelectron. 2011;26(8):3450–5.
[60] Shi W, Liu C, Song Y, Lin N, Zhou S, Cai X. An ascorbic acid amperometric sensor using over-oxidized polypyrrole and palladium nanoparticles composites. Biosens Bioelectron. 2012;38(1):100–6.
[61] Ma Y, Zhao M, Cai B, Wang W, Ye Z, Huang J. 3D graphene foams decorated by CuO nanoflowers for ultrasensitive ascorbic acid detection. Biosens Bioelectron. 2014;59:384–8.
[62] Zaaba NI, Foo KL, Hashim U, Tan SJ, Liu W-W, Voon CH. Synthesis of graphene oxide using modified hummers method: solvent influence. Procedia Eng. 2017;184:469–77.
[63] Ahadian S, Estili M, Surya VJ, Ramón-Azcón J, Liang X, Shiku H, et al. Facile and green production of aqueous graphene dispersions for biomedical applications. Nanoscale. 2015;7(15):6436–43.
[64] Janda P, Weber J, Dunsch L, Lever A. Detection of ascorbic acid using a carbon fiber microelectrode coated with cobalt tetramethylpyridoporphyrazine. Anal Chem. 1996;68(6):960–5.
[65] Luo J, Jiang S, Liu R, Zhang Y, Liu X. Synthesis of water dispersible polyaniline/poly(styrenesulfonic acid) modified graphene composite and its electrochemical properties. Electrochim Acta. 2013;96:103–9.
[66] Sheng Z-H, Zheng X-Q, Xu J-Y, Bao W-J, Wang F-B, Xia X-H. Electrochemical sensor based on nitrogen doped graphene:

simultaneous determination of ascorbic acid, dopamine and uric acid. Biosens Bioelectron. 2012;34(1):125–31.
[67] Zuo X, Zhang H, Li N. An electrochemical biosensor for determination of ascorbic acid by cobalt(II) phthalocyanine-multi-walled carbon nanotubes modified glassy carbon electrode. Sens Actuators B. 2012;161(1):1074–9.
[68] Wang X, Watanabe H, Uchiyama S. Amperometric L-ascorbic acid biosensors equipped with enzyme micelle membrane. Talanta. 2008;74(5):1681–5.
[69] Zhang X, Cao Y, Yu S, Yang F, Xi P. An electrochemical biosensor for ascorbic acid based on carbon-supported PdNi nanoparticles. Biosens Bioelectron. 2013;44:183–90.
[70] Habibi B, Pournaghi-Azar MH. Simultaneous determination of ascorbic acid, dopamine and uric acid by use of a MWCNT modified carbon-ceramic electrode and differential pulse voltammetry. Electrochim Acta. 2010;55(19):5492–8.
[71] Thiagarajan S, Chen S-M. Preparation and characterization of PtAu hybrid film modified electrodes and their use in simultaneous determination of dopamine, ascorbic acid and uric acid. Talanta. 2007;74(2):212–22.
[72] Han D, Han T, Shan C, Ivaska A, Niu L. Simultaneous determination of ascorbic acid, dopamine and uric acid with chitosan-graphene modified electrode. Electroanalysis. 2010;22(17–18):2001–8.
[73] Zheng D, Ye J, Zhou L, Zhang Y, Yu C. Simultaneous determination of dopamine, ascorbic acid and uric acid on ordered mesoporous carbon/nafion composite film. J Electroanal Chem. 2009;625(1):82–7.
[74] Tang C-F, Kumar SA, Chen S-M. Zinc oxide/redox mediator composite films-based sensor for electrochemical detection of important biomolecules. Anal Biochem. 2008;380(2):174–83.
[75] Arvand M, Sohrabnezhad S, Mousavi M, Shamsipur M, Zanjanchi M. Electrochemical study of methylene blue incorporated into mordenite type zeolite and its application for amperometric determination of ascorbic acid in real samples. Anal Chim Acta. 2003;491(2):193–201.
[76] Huang J, Liu Y, Hou H, You T. Simultaneous electrochemical determination of dopamine, uric acid and ascorbic acid using palladium nanoparticle-loaded carbon nanofibers modified electrode. Biosens Bioelectron. 2008;24(4):632–7.
[77] Atta NF, El-Kady MF, Galal A. Simultaneous determination of catecholamines, uric acid and ascorbic acid at physiological levels using poly(*N*-methylpyrrole)/Pd-nanoclusters sensor. Anal Biochem. 2010;400(1):78–88.
[78] Kumar SA, Lo P-H, Chen S-M. Electrochemical selective determination of ascorbic acid at redox active polymer modified electrode derived from direct blue 71. Biosens Bioelectron. 2008;24(4):518–23.
[79] Sun W, Yang M, Gao R, Jiao K. Electrochemical determination of ascorbic acid in room temperature ionic liquid BPPF6 modified carbon paste electrode. Electroanalysis. 2007;19(15):1597–602.
[80] Keeley GP, O'Neill A, McEvoy N, Peltekis N, Coleman JN, Duesberg GS. Electrochemical ascorbic acid sensor based on DMF-exfoliated graphene. J Mater Chem. 2010;20(36):7864–9.
[81] Wu G-H, Wu Y-F, Liu X-W, Rong M-C, Chen X-M, Chen X. An electrochemical ascorbic acid sensor based on palladium nanoparticles supported on graphene oxide. Anal Chim Acta. 2012;745:33–7.